

Remote Sensing Image Fusion Based on Two-stream Fusion Network

Xiangyu Liu¹, Yunhong Wang¹, and Qingjie Liu^{1,2}(✉)

¹ The State Key Laboratory of Virtual Reality Technology and Systems,
Beihang University, Beijing 100191, China

{xyliu, yhwang, qingjie.liu}@buaa.edu.cn

² Beijing Key Laboratory of Digital Media, School of Computer Science and
Engineering, Beihang University, Beijing 100191, China

Abstract. Remote sensing image fusion (or pan-sharpening) aims at generating high resolution multi-spectral (MS) image from inputs of a high spatial resolution single band panchromatic (PAN) image and a low spatial resolution multi-spectral image. In this paper, a deep convolutional neural network with two-stream inputs respectively for PAN and MS images is proposed for remote sensing image pan-sharpening. Firstly the network extracts features from PAN and MS images, then it fuses them to form compact feature maps that can represent both spatial and spectral information of PAN and MS images, simultaneously. Finally, the desired high spatial resolution MS image is recovered from the fused features using an encoding-decoding scheme. Experiments on Quickbird satellite images demonstrate that the proposed method can fuse the PAN and MS image effectively.

1 Introduction

Most remote sensing applications require images at the highest resolution both in spatial and spectral domains which is very hard to achieve by a single sensor. To alleviate this problem, many optical Earth observation satellites, such as QuickBird, GeoEye and IKONOS, carry two kinds of optical sensors, one sensor acquires panchromatic images (PAN) at high spatial and low spectral resolution, the other sensor acquires multi-spectral images (MS) with complementary properties, i.e. low spatial and high spectral resolution. Panchromatic and multi-spectral image fusion (also known as pan-sharpening) aims to fuse information from PAN and MS image to generate images with high spatial and spectral resolutions, simultaneously.

Pan-sharpening can be helpful for a variety of remote sensing applications [26], so it has been raising much attention within remote sensing community. Many methods have been published during the last decade [28]. Most of these methods can be classified into three categories: 1) component substitution (CS) methods; 2) amélioration de la résolution spatiale par injection de structures (ARSIS) concept methods (which means enhancement of the spatial resolution by structure

injections) and 3) model-based methods. The CS methods assume that the geometric detail information of a MS image lies in its structural component which can be obtained by projecting it to a new space. Then, the substitution consists of the total or partial replacement of this structural component by the PAN image. The goal of pan-sharpening can be achieved after an inverse projection. The principal component analysis (PCA) [4], the intensity hue saturation (IHS) [27] and the GramSchmidt (GS) transform [11] based methods are those of the most widely known CS methods. The fundamental assumption of the ARSIS concept methods is that the missing spatial information in MS modalities can be inferred from the high frequencies [22]. To pan-sharpen a MS image, ARSIS methods apply multi-resolution algorithms, such as discrete wavelet transform (DWT) [19], à trous wavelet transform [17] on a PAN image to extract high-frequency information then inject it into a MS image. The model based methods construct a degradation models of how PAN and MS images are degraded from the desired high resolution MS image and restore it from the degradation models [3,31].

In addition to the aforementioned methods, researchers address pan-sharpening from other perspectives. For instance, Li [12] and Zhu [35] model remote sensing image pan-sharpening from compressed sensing theory. He et al. [8] introduced a variational model based on spatial and spectral sparsity priors for pan-sharpening. Liu et al. [13] address pan-sharpening from a manifold learning framework.

Recently, deep learning techniques have been applied to various research fields and achieved astonishing performance [5,9,23,33]. Inspired by SRCNN [5], Masi et al. [16] proposed a pan-sharpening method based on convolutional neural networks (CNNs). They utilized a three-layered CNN architecture modified from [5], which was original designed for image super-resolution. Zhong et al. [34] presented a CNN based hybrid pan-sharpening method. Different from Masi et al.'s method, in [34], CNN was employed to enhance the spatial resolution of the MS image, then the GramSchmidt transform was utilized to fuse the enhanced MS and PAN image to obtain the pan-sharpened image. The network used to enhance the spatial resolution of MS image is also a three-layered CNN same to SRCNN [5].

It has been reported that deeper neural networks can achieve better results than shallow ones [7,9]. And inspired by the tremendous success of deep CNN in image processing and computer vision tasks, in this paper we explore to use a much deeper two streams network to fuse PAN and MS images to generate the desired high resolution MS image. The rest of this paper is organized as follows. Section 2 elaborate our two stream pan-sharpening network. Section 3 gives experiments and comparisons with other methods. Finally, this paper is concluded in Sect. 4.

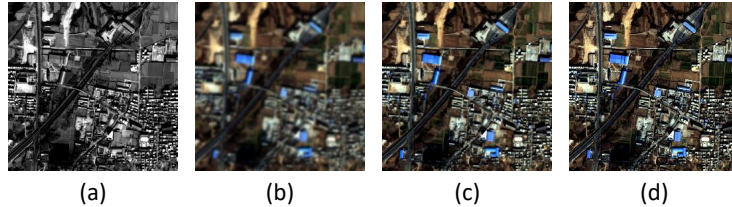


Fig. 1. Example result of the proposed method. The desired high resolution MS image (c) is generated from an input pair of PAN (a) and MS (b). (d) is referenced MS image.

2 Two-stream Fusion Network

The architecture of the proposed Two-stream Fusion Network (TFNet) is shown in Fig. 2. The proposed TFNet consists of three parts, including feature extraction, feature fusion and image restoration.

It is generally accepted that PAN and MS images contain different information. PAN image is carrier of geometric detail (spatial) information, while MS image preserves spectral information. However, it is very hard to define what exactly spatial and spectral information are and how to represent them independently. In this paper, to make the best use of the spatial and spectral information in PAN and MS, we use two sub-networks to extract hierarchical features to capture complementary information of PAN and MS images. We believe the features extracted from PAN and MS contain spatial and spectral information. After feature extraction, the following networks proceed as an auto-encoder, in which the encoder (feature fusion) fuses information extracted from PAN and MS images, then the decoder (image restoration) reconstructs the high resolution MS images from the fused features.

2.1 Feature extraction networks

Pan-sharpening can be considered as a special form of single image resolution [16]. However, the differences between them are obvious. Unlike image super-resolution, pan-sharpening takes two different images, PAN and MS, as input, and produces an image with both characteristics. To reuse the architecture of SRCNN [5], Masi et al. [16] did not consider different information contained in PAN and MS images. They stacked up-sampled MS bands with PAN band to form a five-band image and send it to the network. With our method, the two input images are treated separately. We use two sub-networks to extract features from PAN and MS images respectively. These two sub-networks have similar architecture but different weights. One sub-network takes a 4-band MS image as input and extracts spectral information of it. The other one takes a single band PAN image as input and extract geometric spatial information contained in it.

Each of the sub-networks consists of two successive convolutional layers followed by a leaky rectified linear unit (LeakyReLU) [15] and a down-sampling

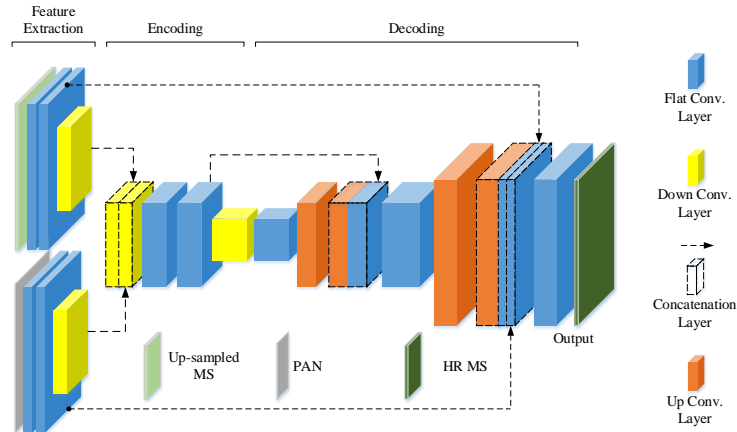


Fig. 2. The architecture of the proposed TFNet.

layer. Most of the CNN architectures utilize max or mean pooling to get scale- and rotational-invariance features, however the detail information is more important in pan-sharpening, so we use the convolutional kernel with a stride of 2 for down-sampling instead of simple pooling strategy.

2.2 Fusion network

After feature extraction, we have two feature maps representing PAN and MS images respectively. The two feature maps explicitly capture complementary information of PAN and MS, i.e. spatial detail and spectral information. Considering that the desired high resolution MS image should have high resolutions both in spatial and spectral, the features of it must describe spatial and spectral information simultaneously. To this end, the two feature maps are concatenated. After that, three convolutional layers are applied to encode the concatenated feature maps into more compact representations. The end of the fusion network is a $[w/4, h/4, 256]^3$ tensor who encodes spatial and spectral information of the two input images.

2.3 Image restoration network

The last stage of the proposed TFNet is reconstructing the desired high resolution MS image from the features. The encoded feature maps only take up 1/16 of the input proportion. One can use traditional method such as linear interpolation to up-sample the scale of feature map. However, learnable way is better [14]. We use backward strided convolutional layers (also known as transposed convolutional layers) to reconstruct the high resolution MS image. Starting with a

³ w and h are the width and height of the input images.

Table 1. The network structure of TFNet.

		Layer	Filter	Stride	Output Size
Input	MS				$128 \times 128 \times 4$
	PAN				$128 \times 128 \times 1$
Feature extraction	MS	FlatConv1_M	$3 \times 3/32$	1	$128 \times 128 \times 32$
		FlatConv2_M	$3 \times 3/32$	1	$128 \times 128 \times 32$
		DownConv3_M	$2 \times 2/64$	2	$64 \times 64 \times 64$
	PAN	FlatConv1_P	$3 \times 3/32$	1	$128 \times 128 \times 32$
		FlatConv2_P	$3 \times 3/32$	1	$128 \times 128 \times 32$
		DownConv3_P	$2 \times 2/64$	2	$64 \times 64 \times 64$
Fusion		Concat1	-	-	$64 \times 64 \times 128$
		FlatConv4	$3 \times 3/128$	1	$64 \times 64 \times 128$
		FlatConv5	$3 \times 3/128$	1	$64 \times 64 \times 128$
		DownConv6	$2 \times 2/256$	2	$32 \times 32 \times 256$
		FlatConv7	$1 \times 1/256$	1	$32 \times 32 \times 256$
		FlatConv8	$3 \times 3/256$	1	$32 \times 32 \times 256$
Restoration		UpConv9	$2 \times 2/128$	2	$64 \times 64 \times 128$
		Concat2	-	-	$64 \times 64 \times 256$
		FlatConv10	$3 \times 3/128$	1	$64 \times 64 \times 128$
		UpConv11	$2 \times 2/64$	2	$128 \times 128 \times 64$
		Concat3	-	-	$128 \times 128 \times 128$
		FlatConv12	$3 \times 3/64$	1	$128 \times 128 \times 64$
		FlatConv13	$3 \times 3/4$	1	$128 \times 128 \times 4$
Output		-	-	-	$128 \times 128 \times 4$

convolutional layer with kernel size of 1×1 applied to combine the feature, we up-sample the feature map every two layers as a symmetrical structure to encoder. Inspired by the skip connection between encoder and decoder utilized in U-Net [24], we also add skip connection between the encoder and decoder of our network. Specifically, after every step of up-sampling, the feature maps in the encoder are copied to the decoder and concatenated with the corresponding feature maps to inject more details lost in down-sampling process, as shown in Fig. 2. In the next section, we will discuss how much performance improvement it will be by adding lower features in the higher level. The last layer outputs the desired high resolution 4-band MS image. Table 1 shows the parameters and details of our network.

3 Experiments

3.1 Dataset

The proposed method is tested on QuickBird images. Quickbird is a commercial satellite launched in October 18, 2001 by DigitalGlobe⁴. Quickbird carries two

⁴ <http://www.digitalglobe.com/>

sensors, one sensor acquires panchromatic images at 0.6 m spatial resolution, and the other sensor acquires 4-band (blue, green, red and near-infrared) multi-spectral images at 2.4 m resolution. Table 2 shows spectral wavelength ranges of different bands.

Table 2. Spectral bands wavelength range (in nanometer) of Quickbird.

	PAN	Blue	Green	Red	Nir
Quickbird	450-900	450-520	520-600	630-690	760-890

The dataset contains 9 pairs of MS and PAN images sized from $558 \times 2080 \times 4$ to $3162 \times 2142 \times 4$ and $2232 \times 8320 \times 1$ to $12648 \times 28568 \times 1$. For each $w \times h$ MS image, there is a corresponding $4w \times 4h$ PAN image over the same site. Our goal is to generate the MS image with the same spatial resolution as the PAN image. To assess the proposed method, the results should be compared with the referenced images, which do not exist. As a conventional method, we follow Wald’s protocol [30] to assess our method and compare it with other methods. That is down-sampling both PAN and MS images by 4 of width and height, separately, then the down-sampled images are used as the inputs of the network and the original MS images are used as references. We also use bi-cubic interpolation algorithm to up-sample the input MS images to match the PANs’ resolution.

3.2 Training

8 out of 9 images are used to train the network and the last one is used to test. The feature extraction net only accepts 128×128 images. we randomly sample 128×128 images from the original and the down-sampled image pairs to form training set. That will generate 64,000 training samples. The cost function is computed over the final output image and the corresponding original MS image with mean square error (MSE). Given a set of original images $\{Y_i\}$ and their corresponding PAN and MS images $\{X_i^P, X_i^M\}$, the MSE is defines as:

$$L(\Theta) = \frac{1}{n} \sum_{i=1}^n \|F(X_i^P, X_i^M; \Theta) - Y_i\|^2 \quad (1)$$

where n is the number of training samples. The loss is minimized using Adam optimizer [10] with a learning rate of 0.0001 and a momentum of 0.5. The mini-batch size is set to 32. The network is implemented in Tensorflow [1] and trained on a NVIDIA Titan-X GPU. It will take about 15 hours to train our network.

3.3 Evaluation indexes

We use five metrics for performance assessment.

Q₄ The Quality-index Q₄ [2] is the 4-band extension of Q index [30], which is defined as:

$$Q_4 = \frac{4|\sigma_{z_1 z_2}| \cdot |\bar{\mathbf{z}}_1| \cdot |\bar{\mathbf{z}}_2|}{(\sigma_{z_1}^2 + \sigma_{z_2}^2)(|\bar{\mathbf{z}}_1|^2 + |\bar{\mathbf{z}}_2|^2)} \quad (2)$$

where z_1 and z_2 are two spectral vectors of MS images, $\bar{\mathbf{z}}_1$ and $\bar{\mathbf{z}}_2$ are the means, $\sigma_{z_1 z_2}$ denotes the covariance between z_1 and z_2 , and $\sigma_{z_1}^2$ and $\sigma_{z_2}^2$ the variances of z_1 and z_2 .

SAM Spectral angle mapper (SAM) [32] is defined as the angular difference between two vectors v_1 and v_2 :

$$\text{SAM}(v_1, v_2) = \arccos\left(\frac{v_1 \cdot v_2}{\|v_1\| \cdot \|v_2\|}\right) \quad (3)$$

where v_1 and v_2 are two spectral vectors of MS images. SAM is averaged over all the images to generate a global measurement of spectral distortion. For the ideal pan-sharpened images, SAM should be zero.

sCC To evaluate the similarity between the spatial details of pan-sharpened images and referenced images, a high pass filter is applied to the images, then the correlation coefficient (CC) between the results is calculated. This quantity index is called spatial CC (sCC). We use the high Laplacian pass filter given by,

$$F = \begin{bmatrix} -1 & -1 & -1 \\ -1 & 8 & -1 \\ -1 & -1 & -1 \end{bmatrix} \quad (4)$$

A higher sCC indicates that most of the spatial information of the PAN image is injected during the fusion process. The final sCC is averaged over all the bands of the MS images.

RASE Relative average spectral error(RASE) is used to estimate the global spectral quality of the fused images[6]. It is defined as

$$\text{RASE} = \frac{100}{M} \sqrt{\frac{1}{N} \sum_{i=1}^N \text{RMSE}^2(B_i)} \quad (5)$$

where N is the number of multi-spectral images, M is the mean radiance of all multi-spectral images, B_i is each multi-spectral image, $\text{RMSE}(B_i)$ is the root mean square error defines as: $\text{RMSE}^2(B_i) = \text{bias}^2(B_i) + \text{SD}^2(B_i)$, where *bias* is the difference between the mean of the referenced image and that of the fused image and *SD* reflects the deviation degree of values relative to the mean of the image.

ERGAS ERGAS is a commonly used global quality index [29], which means relative global dimensional synthesis error. It is given by,

$$\text{ERGAS} = 100 \frac{h}{l} \sqrt{\frac{1}{N} \sum_{i=1}^N \left(\frac{\text{RMSE}(B_i)}{M(B_i)} \right)^2} \quad (6)$$

where h and l are the spatial resolution of PAN and MS images; $\text{RMSE}(B_i)$ is the root mean square error between the i th fused band and the referenced image band; $M(B_i)$ is the mean value of the original MS band B_i .

3.4 Impacts of detail compensation

In order to reconstruct fine details better, as mentioned in Sect. 2.3, we concatenate the low-level feature maps with the corresponding high level feature maps in the same resolution after every up-sampling step. Since PAN images carry spatial detail information, it is reasonable to employ features of PAN to compensate spatial information. An alternative solution is compensating features from both PAN and MS images to the corresponding high level feature maps of restoration network. Surprisingly, the latter one achieves better results in terms of both spatial and spectral qualities than the first one shown in Table 3. The reason behind this may be that both PAN and MS images contains spatial and spectral information. It is impossible to separate spatial and spectral information from each other and extract only spatial details from PAN image or spectral features from MS images. To get better results, one should not focus only on how to extract spatial or spectral information separately. Both PAN and MS images should be taken into consideration.

Table 3. Performance of different concatenation strategies

	Q ₄	ERGAS	RASE	sCC	SAM
None	0.9370	7.4561	29.1958	0.9596	3.9598
PAN	0.9438	6.7348	25.8415	0.9603	3.3653
MS&PAN	0.9576	6.2010	23.9232	0.9625	2.8762

3.5 Comparison with other methods

In this subsection we compare the proposed method with several widely used techniques.

- APCA: Adaptive Principal Components Analysis [25].

- AIHS: Adaptive Intensity-Hue-Saturation [21].
- AWLP: Additive Wavelet Luminance Proportional [18].
- PNN: CNN-based Pan-sharpening [16].

We re-implement the first four techniques in MATLAB, and [16] with Tensorflow with the same hyper-parameters. Table 4 shows the results in terms of four evaluation metrics. Additionally, we provide the performance using simple nearest neighbor interpolation (EMS) as the baseline [20].

Table 4. Performance comparison on the test dataset

	Q ₄	ERGAS	RASE	sCC	SAM
EMS [20]	0.7687	13.6148	50.8050	0.8169	6.3484
APCA [25]	0.8590	11.8154	44.1160	0.9086	5.5634
AIHS [21]	0.8408	11.0549	41.3064	0.9156	5.0821
AWLP [18]	0.9021	11.7006	41.0487	0.9145	4.7441
PNN [16]	0.9511	6.7531	25.6368	0.9567	3.0481
TFNet	0.9576	6.2010	23.9232	0.9625	2.8762

From Table 4 we can see that the proposed methods guarantee performance gains on all the metrics. One can notice that our method is much better than traditional methods of PACA [25], AIHS [21] and AWLP [18]. When compared with recently proposed PCNN, which is a three-layer convolutional model, our method also has significant advantages in spectral reconstruction and detail preservation. In Figs. 3 and 4, we show the results of different techniques on Quickbird. The pan-sharpened images generated by the proposed method look better. APCA and AIHS produce images with obvious blurring. AWLP returns images similar to the reference images with fine spatial details, but suffers from strong spectral distortions. PNN’s results are similar to the proposed method. Some missing spatial details are noticeable. The proposed method does better in spectral preservation and provides images with richer spatial details.

4 Conclusion

Deep learning has been drawing increasing attention from both computer vision and remote sensing communities. Significant progresses have been achieved in computer vision and image processing field, yet in remote sensing tasks there are still great advances to achieve with the help of deep learning techniques. Based on the intuition that, the high resolution MS image should have same features

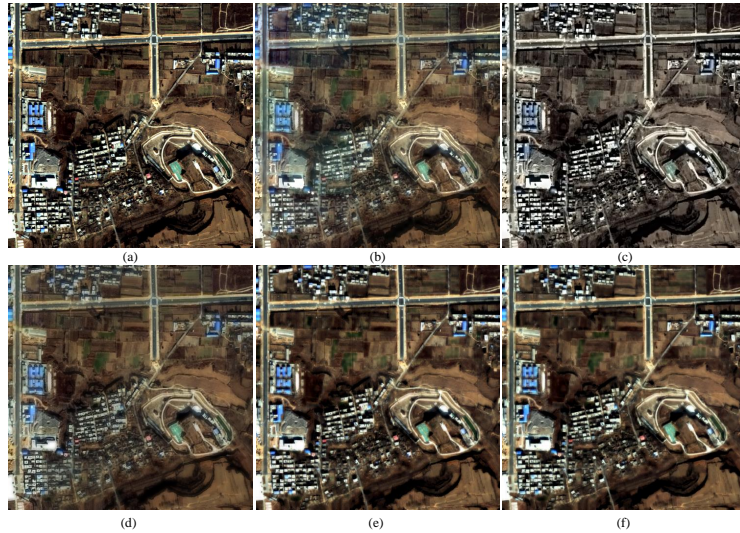


Fig. 3. Pansharpening results on the Quickbird images. (a) Referenced Image; (b) APCA [25]; (c) AWLP [18]; (d) AIHS [21]; (e) PNN [16] and (f) the proposed TFNet. Displayed in true color (RGB).

as that of PAN and MS images. In this paper, we propose a two-stream pansharpening network like autoencoder that extracts features from PAN and MS respectively. Encoding and decoding scheme is applied to fuse features together and reconstruct the high resolution MS images. The experiments on Quickbird images demonstrate the effectiveness of the proposed method and comparisons with other methods also shows superiority of our method.

Acknowledgments This work is supported by the Natural Science Foundation of China (NSFC) under Grant No. 61601011. Qingjie Liu is corresponding author of this paper.

References

1. Abadi, M., Agarwal, A., Barham, P., Brevdo, E., Chen, Z., Citro, C., Corrado, G.S., Davis, A., Dean, J., Devin, M., et al.: Tensorflow: Large-scale machine learning on heterogeneous distributed systems. arXiv preprint arXiv:1603.04467 (2016)
2. Alparone, L., Baronti, S., Garzelli, A., Nencini, F.: A global quality measurement of pan-sharpened multispectral imagery. *GRSL* 1(4), 313–317 (2004)
3. Aly, H.A., Sharma, G.: A regularized model-based optimization framework for pan-sharpening. *TIP* 23(6), 2596–2608 (2014)
4. Chavez, P., Sides, S.C., Anderson, J.A., et al.: Comparison of three different methods to merge multiresolution and multispectral data- Landsat TM and SPOT panchromatic. *PE&RS* 57(3), 295–303 (1991)

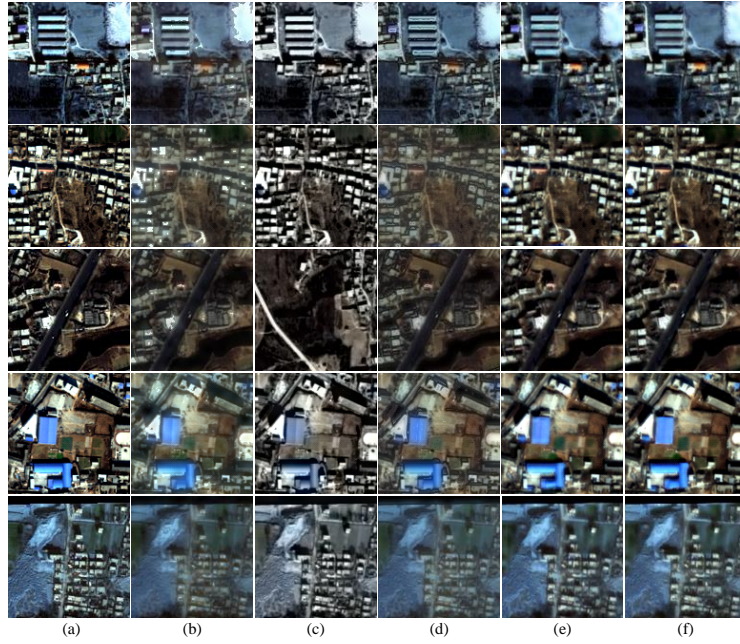


Fig. 4. Sub-regions of the results. (a) Referenced Image; (b) APCA [25]; (c) AWLP [18]; (d) AIHS [21]; (e) PNN [16] and (f) the proposed TFNet. Better viewed in color.

5. Dong, C., Loy, C.C., He, K., Tang, X.: Image super-resolution using deep convolutional networks. *TPAMI* 38(2), 295–307 (2016)
6. González-Audícana, M., Saleta, J.L., Catalán, R.G., García, R.: Fusion of multi-spectral and panchromatic images using improved ihs and pca mergers based on wavelet decomposition. *TGRS* 42(6), 1291–1299 (2004)
7. He, K., Zhang, X., Ren, S., Sun, J.: Deep residual learning for image recognition. In: *CVPR*. pp. 770–778 (2016)
8. He, X., Condat, L., Bioucas-Dias, J.M., Chanussot, J., Xia, J.: A new pansharpening method based on spatial and spectral sparsity priors. *TIP* 23(9), 4160–4174 (2014)
9. Kim, J., Kwon Lee, J., Mu Lee, K.: Accurate image super-resolution using very deep convolutional networks. In: *CVPR*. pp. 1646–1654 (2016)
10. Kingma, D., Ba, J.: Adam: A method for stochastic optimization. *arXiv preprint arXiv:1412.6980* (2014)
11. Laben, C.A., Brower, B.V.: Process for enhancing the spatial resolution of multi-spectral imagery using pan-sharpening (Jan 4 2000), US Patent 6,011,875
12. Li, S., Yang, B.: A new pan-sharpening method using a compressed sensing technique. *TGRS* 49(2), 738–746 (2011)
13. Liu, Q., Wang, Y., Zhang, Z.: Pan-sharpening based on geometric clustered neighbor embedding. *OE* 53(9), 093109–093109 (2014)
14. Long, J., Shelhamer, E., Darrell, T.: Fully convolutional networks for semantic segmentation. In: *CVPR*. pp. 3431–3440 (2015)

15. Maas, A.L., Hannun, A.Y., Ng, A.Y.: Rectifier nonlinearities improve neural network acoustic models. In: ICML. vol. 30 (2013)
16. Masi, G., Cozzolino, D., Verdoliva, L., Scarpa, G.: Pansharpening by convolutional neural networks. *Remote Sens.* 8(7), 594 (2016)
17. Nunez, J., Otazu, X., Fors, O., Prades, A., Pala, V., Arbiol, R.: Multiresolution-based image fusion with additive wavelet decomposition. *TGRS* 37(3), 1204–1211 (1999)
18. Otazu, X., González-Audícana, M., Fors, O., Núñez, J.: Introduction of sensor spectral response into image fusion methods. application to wavelet-based methods. *TGRS* 43(10), 2376–2385 (2005)
19. Pradhan, P.S., King, R.L., Younan, N.H., Holcomb, D.W.: Estimation of the number of decomposition levels for a wavelet-based multiresolution multisensor image fusion. *TGRS* 44(12), 3674–3686 (2006)
20. Prashanth, H., Shashidhara, H., KN, B.M.: Image scaling comparison using universal image quality index. In: IAC3T. pp. 859–863. IEEE (2009)
21. Rahmani, S., Strait, M., Merkurjev, D., Moeller, M., Wittman, T.: An adaptive ihs pan-sharpening method. *GRSL* 7(4), 746–750 (2010)
22. Ranchin, T., Wald, L.: Fusion of high spatial and spectral resolution images: The arsis concept and its implementation. *PE&RS* 66(1), 49–61 (2000)
23. Ren, S., He, K., Girshick, R., Sun, J.: Faster r-cnn: Towards real-time object detection with region proposal networks. In: NIPS. pp. 91–99 (2015)
24. Ronneberger, O., Fischer, P., Brox, T.: U-Net: Convolutional networks for biomedical image segmentation. In: MICCAI. pp. 234–241. Springer (2015)
25. Shah, V.P., Younan, N.H., King, R.L.: An efficient pan-sharpening method via a combined adaptive PCA approach and contourlets. *TGRS* 46(5), 1323–1335 (2008)
26. Thomas, C., Ranchin, T., Wald, L., Chanussot, J.: Synthesis of multispectral images to high spatial resolution: A critical review of fusion methods based on remote sensing physics. *TGRS* 46(5), 1301–1312 (2008)
27. Tu, T.M., Su, S.C., Shyu, H.C., Huang, P.S.: A new look at ihs-like image fusion methods. *INFORM FUSION* 2(3), 177–186 (2001)
28. Vivone, G., Alparone, L., Chanussot, J., Dalla Mura, M., Garzelli, A., Licciardi, G.A., Restaino, R., Wald, L.: A critical comparison among pansharpening algorithms. *TGRS* 53(5), 2565–2586 (2015)
29. Wald, L.: Quality of high resolution synthesised images: Is there a simple criterion? In: Proceedings of the Fusion of Earth Data: Merging Point Measurements, Raster Maps, and Remotely Sensed image (2000)
30. Wald, L., Ranchin, T., Mangolini, M.: Fusion of satellite images of different spatial resolutions: Assessing the quality of resulting images. *PE&RS* 63, 691–699 (1997)
31. Wei, Q., Dobigeon, N., Tourneret, J.Y.: Bayesian fusion of multi-band images. *J-STSP* 9(6), 1117–1127 (2015)
32. Yuhas, R.H., Goetz, A.F.H., Boardman, J.: Discrimination among semi-arid landscape endmembers using the spectral angle mapper (SAM) algorithm. In: Proc. Summaries 3rd Annu. JPL Airborne Geosci. Workshop. pp. 147 – 149 (Jun 1992)
33. Zhang, Q., Wang, Y., Liu, Q., Liu, X., Wang, W.: CNN based suburban building detection using monocular high resolution google earth images. In: IGARSS. pp. 661–664. IEEE (2016)
34. Zhong, J., Yang, B., Huang, G., Zhong, F., Chen, Z.: Remote sensing image fusion with convolutional neural network. *Sensing and Imaging* 17(1), 10 (2016)
35. Zhu, X.X., Bamler, R.: A sparse image fusion algorithm with application to pansharpening. *TGRS* 51(5), 2827–2836 (2013)